

Determinate Chloride Diffusion Coefficient and Corrosion Initiation on Self-consolidating Concrete

Experimental and Numerical Approaches

Shahram TaleshAbedini¹, Hossein Rahami^{2*}, Seyed Mohammad Mir Hosseini¹, Ehsanollah Zeighami¹

¹ Department of Civil Engineering, Arak Branch, Islamic Azad University, 3rd km of Khomein road, Arak, Iran

² School of Engineering Science, College of Engineering, University of Tehran, North Kargar st., Tehran, Iran

* Corresponding author, e-mail: hrahami@ut.ac.ir

Received: 30 January 2024, Accepted: 06 January 2025, Published online: 10 February 2025

Abstract

The use of supplementary cementitious materials (SCMs) such as silica fume (SF), metakaolin (MK), fly ash (FA), and slag (SL) can significantly extend concrete life, especially for those exposed to coastal environments. An essential part of estimating the service life of the reinforced concrete (RC) structures is estimating the time when the corrosion begins. The diffusion coefficient that leads to the concentration of chloride ions in concrete is one of the most important parameters for evaluating the corrosion initiation time. This study determined the chloride diffusion coefficient by preparing samples containing different admixtures based on the Nord-test accelerated migration test. The samples are placed in two environmental conditions, submerged and dry and wet cycles for 180 days. The Charged System Search (CSS) meta-exploration algorithm based on the Hesofer-Lind-Rakowitz-Fissler (HL-RF) method evaluated corrosion and chloride diffusion coefficient initiation time. Test results and numerical models showed that in a sample with admixture, its corrosion resistance was almost two times that of the ordinary concrete and the initial corrosion time. If several types of admixture are used, the corrosion time becomes twice as long as when only one admixture is utilized. The best performance for the durability of concrete belonged to the samples with three admixtures. Using additives, MK, SF, and SL, with concrete results in the probability of corrosion to decrease by about 40% after 25 years, and at 50 years, this value becomes about 50%.

Keywords

mineral admixture, diffusion coefficient test, corrosion initiation, durability design

1 Introduction

Considering the widespread use of cement-based materials in structures, more than ten billion tons of concrete are produced annually [1], responsible for 9% of global industrial water [2]. Corrosion of reinforcements in reinforced concrete (RC) structures significantly affects RC structures' durability [3]. For this purpose, mineral admixture can replace materials utilized in concrete manufacturing, reduce the adverse effects on the environment, and increase durability [4, 5]. Furthermore, governments spend considerable expenses on the maintenance of corroded structures [6, 7]. In this regard, chloride-induced corrosion captivates great attention among researchers [8–10]. The normal alkalinity of concrete is PH of about 13, which protects the rebars against chloride via an iron oxide layer called a passive layer. However, the reduction in PH level, especially for carbonation or chloride ingress of the

concrete, destroys the passive layer of concrete, leading to rebar corrosion [11]. Chloride ions are not bonded and combined in the corrosion process. In other words, they act like catalysts, which means they help break the steel oxide layer and cause the corrosion process's rapid progress [12].

During the corrosion process, the corrosion products gather on the surfaces of the rebar and start to fill the pores in the concrete [13]. Research studies have shown this feeling leads to excessive-stress levels [14]. These excessive stresses can result in longitudinal cracks running parallel to the reinforcements and, in some cases, delamination and splitting of the concrete [15–19], which can shorten the structural capacity and service life [20, 21]. So, de-passivation leads to the end of the structures' service life [22, 23]. Also, mineral admixtures instead of cement have been considered in recent years to increase

the durability of concrete structures and the longer life of these devices [14, 24].

Sell Junior et al. [24] investigated the effect of the water-cement ratio and the use of silica fume (SF) in amounts of 5, 10, and 20% on the resistance of concrete against concrete penetration, and the results indicate that increasing the water-cement ratio increases the chloride ion penetration coefficient it becomes concrete. Also, increasing the amount of SF used in concrete increases the resistance of concrete against chloride penetration. The lowest chloride penetration coefficient is related to concrete containing the highest amount of SF. Khanzadeh Moradllo et al. [25] investigated the effect of metakaolin (MK) at 5, 10, and 15% on chloride ion permeability, and the results show that increasing the amount of MK increases the resistance of concrete against chloride penetration. Also, in research conducted by Ramezani pour et al. [26], it has been observed that using calcined clay and stone powder as a substitute for cement reduces the permeability of concrete against chloride ions and increases the resistance of concrete against chloride penetration. Similarly, Shafikhani and Chidiac [27] found that using ground granulated blast-furnace slag (GGBFS) and fly ash (FA) as a cement substitute increases concrete resistance against chloride penetration and decreases the permeability of concrete. Also, the simultaneous use of these two types of admixtures reduces the permeability coefficient of concrete. The use of minerals increases the resistance of concrete against chloride ion penetration due to the pozzolanic reaction that is effective in forming calcium hydro silicate (C-S-H) secondary gel. Due to the smaller size of these materials compared to cement, the amount of pores in concrete will be less, which increases the permeability of concrete decreases.

According to the results obtained from the investigated research, using mineral materials as an alternative to cement reduces the penetration coefficient of chloride in concrete and, as a result, increases the structure's lifetime. Since the minerals used in the presented research are often used singly and in limited proportions, this research examined the

effect of various minerals, such as SF, MK, and slag (SL), on the chloride permeability coefficient singly and in combination. The samples were subjected to two different environmental conditions. Group A was fully exposed, while group B underwent 60 cycles of drying-wetting conditions for 180 days. At the end of 28 and 120 days, the diffusion coefficient of chloride in concrete was determined. The durability of samples against chloride corrosion was calculated with an effective metaheuristic algorithm named Charged System Search (CSS) that is compatible with durability design problems of samples based on the Hesofer-Lind-Rakowitz-Fissler (HL-RF) method.

2 Methodology

2.1 Materials properties

To conduct tests and studies on the effect of mineral admixtures on the chloride diffusion coefficient of self-compacting concrete, samples were made with different supplementary cementitious materials (SCMs) (SL, MK, and SF). The composition of the SCMs and cement was determined by X-ray fluorescence (XRF) and is shown in Table 1.

2.2 Mixed design proportions

The water-to-binder (W/B) ratio for product concrete samples is 0.4. The details of the mixing plan are presented in Table 2 (where SCC is the self-consolidating concrete). In all the samples, the total volume of aggregate materials was considered equal to 0.627, and the volume ratio of sand to stone materials was considered constant at 0.65. In addition, the volume ratio of fine sand to coarse was also considered 1 to 2. The cement used in all designs is ordinary Portland cement (PC) (Type II with C_3A equal to 4.98%), whose specifications are presented in Table 1. Coarse stone grains (sand) of stone broken with a maximum nominal size of 19 mm and a specific weight of 2.65 were used. Aggregate materials under sand grains with a modulus of softness of 2.65 and a specific gravity of 2.6 were used. The sand water absorption is 0.039, based on the humidity measured in the workshop in each

Table 1 Chemical composition of materials measured by XRF (mass %)

Material	Chemical composition								Specific surface area (m ² /kg)	Density (kg/m ³)
	SiO ₂	MgO	Al ₂ O ₃	Fe ₂ O ₃	CaO	Na ₂ O	K ₂ O	LOI		
Cement	21.83	2.15	4.85	3.62	65.89	0.11	0.63	0.92	365	3115
SL	35.65	4.14	15.22	1.42	41.02	0.69	1.03	0.83	396	2285
MK	71.89	0.76	19.78	1.62	3.42	1.04	0.92	0.57	982	2525
SF	95.31	0.43	1.47	1.41	0.63	0.31	0.45	0.44	18750	1400

Table 2 Details of each mixing plan (kg/m³)

Mix name	SF	MK	SL	Cement	W/B	Limestone powder (L_p)	Aggregate volume (m ³)	Superplasticizer (% cement weight)
SCC	–	–	–	400		180		0.34
SL	–	–	200	200		165		0.54
MK	–	80	–	320		175		0.62
SF	32	–	–	368	0.4	175	0.625	0.51
SL+MK	–	80	200	120		170		0.63
SL+SF	32	–	200	168		165		0.6
MK+SF	32	80	–	288		175		0.59
SL+MK+SF	32	80	200	88		160		0.65

construction; the necessary corrections to the consumption values have been made. Coarse sand and fine sand, as well as coarse and fine sand, were selected in equal amounts. A super lubricant was used to keep the slump stable.

As shown in Table 2, the minerals used as cement substitutes include SF, MK, and SL. The first sample is normal concrete, the second contains 50% SL, the third includes 20% MK, and the fourth contains approximately 8% SF. Also, the fifth sample comprises 50% SL and 20% MK, the sixth sample has 50% SL and 8% SF, the seventh sample includes 20% MK and 8% SF, and finally, the eighth sample contains 50% the percentage of SL, 20% of MK and 10% of SF is at the same time.

2.3 Preparation samples

To perform the tests, for each mixture design, six specimens with dimensions 100 × 100 × 100 millimeters were made for compressive strength tests, and six cylindrical samples were made for rapid chloride migration test (RCMT). Cylindrical samples were made to investigate chloride ion penetration rate under accelerated test based on RCMT standard and NT-build code 492 [28]. After pouring concrete into the mold and vibrating, the samples are kept in the mold for 24 h, and then they are kept in the water tank for 28 days with a constant temperature of approximately 22 ± 2 °C and humidity near 95 ± 2% (Fig. 1).

2.4 The corrosion environment

The cured samples were divided into two groups. Group A was immersed in a 5% NaCl solution at room temperature,



Fig. 1 Samples in the first series of production

while group B was exposed to dry-wet circulation and NaCl solution erosion. The concentration of NaCl in both groups was kept constant by replacing the solution every 30 days. The treatment of group B samples followed the GB/T 50082-2009 standard [29] and involved the following steps:

1. Soak the cured sample in sodium chloride at 25 °C for 48 h.
2. Remove the solution and air dry the sample for 1 h.
3. Dry the sample at 60 °C for 24 h.
4. Cool the sample by air for 1.5 h after drying.

2.5 Diffusion coefficient of concrete containing SCMs

The lifespan of RC structures is determined by various concrete properties, including porosity, permeability, mix design, admixture effects, water-cement ratio (W/C), water-binder ratio (W/B), cover thickness, and environmental conditions. This lifespan is calculated using Fick's second law, which assumes that the concrete medium is homogeneous and isotropic [30, 31]. The solution to Eq. (1) will result in $C(x,t)$:

$$C(x,t) = C_s \left[1 - \operatorname{erf} \left(\frac{x}{2\sqrt{Dt}} \right) \right], \quad (1)$$

where $C(x,t)$ is the chloride ion concentration at depth x after t days, determining corrosion initiation is considered as C_{th} or chloride threshold in limit state function, C_s is the surface chloride concentration, and $\operatorname{erf}(\cdot)$ is the error function. The chloride diffusion coefficient is represented by D , the time by t , and the depth from the concrete surface by x . The initial conditions, as defined in [32, 33], are as follows: At time $t = 0$, the chloride concentration is 0, and the chloride concentration on the surface remains constant. Riding et al. [34] proposed a concrete diffusion coefficient considering the SCMs effect:

$$D = D_{28} \left(\frac{t_{28}}{t} \right)^m + D_{ult} \left(1 - \left(\frac{t_{28}}{t} \right)^m \right), \quad (2)$$

where D is the apparent diffusion coefficient, t_{28} is 28 days, m is the decay constant that for Portland concrete is considered 0.264 according to [30].

$$D = D_{28} = 2.17 \times 10^{-12} e^{\left(\frac{w/cm}{0.279}\right)} \quad (3)$$

$$D_{ult} = \left(D_{28} \left(\frac{28}{36500} \right)^m \right) \quad (4)$$

The decay diffusion coefficient for 50% of FA and 70% of SL are 0.69 and 0.62, respectively. (FA and SL represent contents in per cents):

$$m = 0.26 + 0.4 \left(\frac{FA}{50} + \frac{SG}{70} \right). \quad (5)$$

It is assumed that SF and MK do not affect the decay coefficient, so the decay coefficient for these SCMs is the same as that of normal concrete and equal to 0.264. On the other hand, these SCMs' effect on the D_{28} is as follows:

$$\frac{D_{SF}}{D_{PC}} = 0.206 + 0.794 e^{\left(\frac{-SF}{2.51}\right)}, \quad (6)$$

$$\frac{D_{MK}}{D_{PC}} = 0.170 + 0.829 e^{\left(\frac{-MK}{6.12}\right)}. \quad (7)$$

2.6 Reliability-based approach and the analysis method

In the probabilistic approach, uncertainties such as loads, material properties, etc., are considered random variables. The main objective of reliability analysis is to determine the probability of failure. To start, a set of random variables $X = \{X_1, X_2, \dots, X_n\}$ representing uncertainties needs to be identified. A statistical distribution should also be chosen for each random variable to define their randomness. It's important to note that these statistical distributions can be determined through various methods, such as experimental investigations, physical observations, or statistical studies. The structural condition is then evaluated based on the probability of failure, P_f . To calculate P_f , the failure condition must be defined as a function of the random variables, referred to as a limit state function. A limit state represents the boundary between the desired state and failure [35, 36]:

$$g(X) = R(X) - S(X), \quad (8)$$

$$P_f = P[g(X) < 0], \quad (9)$$

where R represents the resistance, and S represents the system's loading. R and S are functions of random variables X .

Understanding the notation $g(X) < 0$, which indicates the failure region, is crucial. Statistical information about specific quantities may not always be available, so describing them in a probabilistic model is necessary. Typically, the obtained P_f value indicates the trend of deterioration over a specific period [37]. In this context, Eq. (11) represents the limit state function.

$$g(X) = C_{th} - C(x, t) \quad (10)$$

Equation (10) specifies that C_{th} denotes the critical value for chloride concentration on the reinforcement surface, while $C(x, t)$ signifies the chloride concentration at depth x at time t . Therefore, chloride limited state function is written as:

$$g(x, t) = C_{th} - C_s \left[1 - \operatorname{erf} \left(\frac{x}{2\sqrt{Dt}} \right) \right]. \quad (11)$$

The reliability index stands at the forefront of reliability analysis and calculation. According to the HL-RF definition, the reliability index (β) represents the closest distance between a surface of the limited state function and the coordinate origin in normal standard space (U space) [38, 39]. With this definition, the corresponding point of the reliability index is known as the design point (DP). Therefore, the process of calculating the reliability index and determining the DP presents itself as an optimization problem, taking the following mathematical form:

$$\begin{aligned} & \text{Minimize } \beta(u) = (u^T u)^{\frac{1}{2}} \\ & u = [u_1, u_2, \dots, u_n]; u_i \in U, \\ & \text{Subject to: } G(u) = 0 \end{aligned} \quad (12)$$

where u_i is the corresponding value of the transferred DP of every parameter to the standard normal space.

In simple terms, when all of the variables follow the normal distribution and are independent from each other, the failure probability is calculated as follows:

$$P_f = \Phi(-\beta), \quad (13)$$

where $\Phi(\beta)$ is the cumulative distribution function, and β is the safety or reliability index.

Considering that premature estimation of corrosion leads to an uneconomic design and late estimation of the actual design period causes an unsafe design, it is essential to calculate the exact time of the beginning of corrosion [40].

In this study, the CSS method is used to find the design and calculation point of the reliability index. The CSS method is a population-based meta-heuristic algorithm introduced by Kaveh et al. [41] and used for the numerical

solution of the durability of RC against carbonation and chloride ingress [40]. In this model, the corrosion probability for durability problems is calculated and presented using two methods of CSS and Monte Carlo simulation with simulations. The model for calculating durability and corrosion has been developed, and its effectiveness has been proven compared to Monte Carlo modeling. In addition, it has a much higher speed in convergence and reaching the answer. The correct estimation of the corrosion start time in RC structures requires the determination of D , which in this research is calculated according to the type of additive used in concrete. Of course, some other parameters, such as geometric dimensions and cross-sectional characteristics, such as rebars and concrete cover, as well as the environmental conditions of the placement of the RC structure, play an essential role in calculating the structure's lifespan.

2.7 Chloride ion diffusion coefficient test (RCMT test)

One of the methods that has shown good compliance with the results of long-term methods is the accelerated chloride ion migration (RCMT) method. This method is based on [28] and is generally similar to the Rapid Chloride Permeability Test (RCPT) method. Still, in this method, the voltage applied to the sample changes according to the current passing through it, and the volume of the salt solution in contact with the sample increases significantly.

In this article, the preparation method is similar to RCPT. In this way, after being saturated with water, the samples are placed inside the plastic sheath, and their peripheral surface is isolated; then, soda solution with a concentration of 0.3 average is poured into the rubber sheath, and the upper face of the concrete specimen is in contact. The prepared set is placed in a container containing a salt solution with a concentration of 10% so that the lower side of the sample is in contact with the salt solution (Fig. 2). After the tests, diluting the samples, and spraying 0.1 M silver nitrate on the samples, the penetration rate and, of course,



Fig. 2 The shape of the samples connected to the accelerated chloride permeation device in the laboratory

the diffusion coefficient will be determined. Non-steady-state migration coefficient calculated from Eq. (14):

$$D_{nssm} = \frac{RT}{zFE} \times \frac{x_d - \alpha \sqrt{x_d}}{t}, \quad (14)$$

where:

$$E = \frac{U - 2}{L}, \quad (15)$$

$$\alpha = 2 \sqrt{\frac{RT}{zFE}} \times \text{erf}^{-1} \left(1 - \frac{2c_d}{c_0} \right). \quad (16)$$

In Eqs. (14) to (16), D_{nssm} is the non-steady-state migration coefficient, z is the absolute value of ion valence, for chloride $z = 1$, F is the Faraday constant (9.648×10^4 J (K mol)), E is the intensity of the electric field, U is the absolute value of the applied voltage (V), R is the Gas constant (8.314 J (K mol)), L is the thickness of the specimen (mm), T is the average value of the initial and final temperatures in the anolyte solution ($^{\circ}\text{C}$), x_d is the average value of the penetration depths (mm), t is the test duration (s), erf^{-1} is the inverse of the error function, c_d is the chloride concentration at which the color changes ($c_d = 0.07$ N for ordinary Portland cement (OPC) concrete), and c_0 is the chloride concentration in the catholyte solution ($c_0 = 2$ N). Since $\text{erf}^{-1} (1 - 2 \times 0.07/2) = 1.28$ the following simplified equation (Eq. (17)) can be used:

$$D_{nssm} = \frac{0.0239(273+T)L}{(U-2)t} \left(x_d - 0.0238 \sqrt{\frac{(273+T)Lx_d}{U-2}} \right), \quad (17)$$

where D_{nssm} is the non-steady-state migration coefficient ($\times 10^{-12}$ m²/s), U is the absolute value of the applied voltage (V), T is the average value of the initial and final temperatures in the anolyte solution ($^{\circ}\text{C}$), L is the thickness of the specimen (mm), x_d is the average value of the penetration depths (mm), t is the test duration (hour). Therefore, having the penetration depth in millimeters, the value of the diffusion coefficient of the unstable state can be calculated. Fig. 2 illustrates the experimental procedures conducted in the laboratory.

3 Result and discussion

3.1 Workability of fresh self-compacting concrete

The fresh mixture workability results are presented in Table 3. The addition of mineral admixtures (such as SSF, MK, and SL) to the mixtures resulted in increased V -funnel

Table 3 The workability results of all SCC mixtures

Specimen name	Slump flow		<i>V</i> -funnel (s)	<i>J</i> ring (mm)	<i>L</i> box h2/h1
	Slump flow (mm)	<i>T</i> ₅₀			
Control specimen	720	3.2	5.1	4	0.94
SL	680	4.9	7.8	8	0.91
MK	690	4.2	7.1	5	0.93
SF	700	4.2	6.9	6	0.95
SL+MK	650	6.3	10.5	7	0.90
SL+SF	670	6.0	11.1	8	0.93
MK+SF	690	5.5	9.4	7	0.91
SL+MK+SF	680	7.8	11.2	9	0.88

and *T*₅₀ times, indicating improved adhesive characteristics of the mix with these materials. This increase was more pronounced when a combination of mineral admixtures was used. Additionally, the results indicated that the use of mineral admixtures could enhance the visual stability index (VSI) of SCC.

3.2 Compressive strength analysis

The compressive strength of the samples made for each mixture design in groups A and B is shown in Fig. 3. Three samples are tested for each time step, and their average is reported based on the standard BS EN 12390-3:2002 [42]. Fig. 3 (a) indicates that the compressive strength containing cement additives for MK, SF, MK+SF, and SL+MK+SF samples performs better than the SCC sample. This issue is more related to the decrease in the permeability of the samples and the formation of the C-S-H gel. The results of group A are higher than the results of group B, which is due to the effect of drying and wetting cycles, which increases the penetration rate in the samples, which results in the growth of micro-cracks and a decrease in compressive strength and useful life of the concrete sample. As shown in Fig. 3 (a) and (b), the sample containing all three supplementary cement materials (SL+MK+SF) has the highest compressive strength, which increases by 20% and 10% for groups A and B, respectively.

3.3 Penetration of chloride in SCC

According to the applied constant potential difference, the current passing through each sample was recorded in short periods. In Table 4, the resistance of different samples against corrosion is presented by measuring the passing current at the constant applied voltage at other times. For each sample, based on the initial passing current at a voltage of 30 volts, according to [28], the amount of voltage and the time of applying the current were determined. The unsteady state diffusion coefficient was calculated based on the average

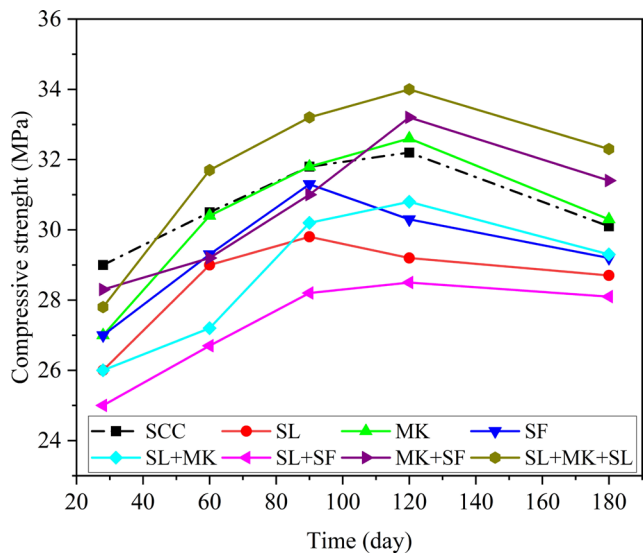
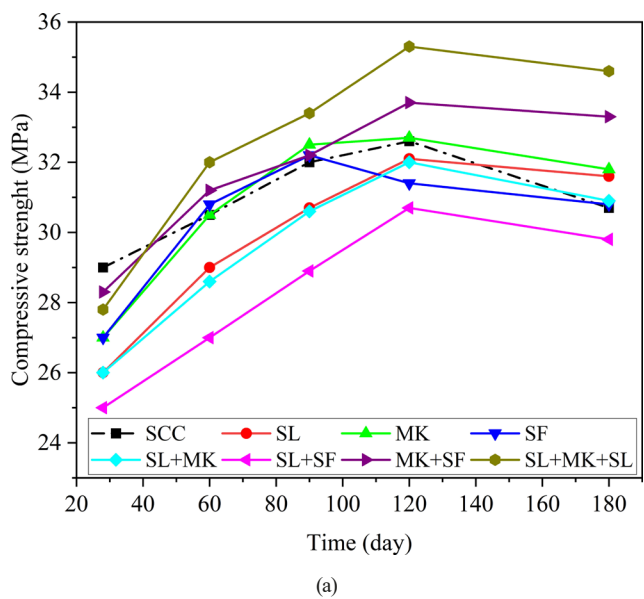


Fig. 3 Compressive strength of the samples for: (a) Group A, (b) Group B

penetration depth calculated for each sample. The average was reported to have six samples for each sample.

Table 4 Determination of diffusion coefficient of the samples after 28 and 120 days

Mix name	Mean of penetration – 28 days (mm)	Mean of D_{nssm} – 28 days (10^{-12} m ² /s)	Mean of penetration – 120 days (mm) – Group (A)	Mean of D_{nssm} – 120 days (10^{-12} m ² /s) – Group (A)	Mean of penetration – 120 days (mm) – Group (B)	Mean of D_{nssm} – 120 days (10^{-12} m ² /s) – Group (B)
SCC	9.8	2.57	30.4	1.15	50	24
SL	7.3	1.57	21.5	0.64	50	24
MK	5.7	1.20	18.5	0.58	50	24
SF	5.5	1.16	16.3	0.51	50	24
SL+MK	6.7	0.72	13.2	0.27	43	19
SL+SF	6.4	0.68	9.8	0.25	41	18
MK+SF	6.3	0.67	5.2	0.21	44	20
SL+MK+SF	4.3	0.22	1.8	0.08	19	7

According to the results, it can be seen that increasing the curing time from 28 to 120 days will increase the resistance to chloride ion diffusion and penetration by almost two times. With the completion of the cement hydration processes and the pozzolans used, the formed materials will essentially prevent the penetration of chlorides.

The use of SL, MK, and SF increases the resistance of concrete against chloride ion penetration due to the pozzolanic reaction that is effective in forming C-S-H secondary gel. Moreover, due to the smaller size of these materials compared to cement, the number of pores in concrete will be less, increasing the permeability of concrete. Using SCMs together as a cement replacement increases concrete permeability more than concrete containing one SCMs since the ratio of replacement increases. In the samples containing SCMs, it was observed that the penetration resistance is not directly related to the compressive strength. Figs. 4 and 5 show the penetration rate at the end of 120 days for both groups, A and B, according to the results obtained in Table 4. Fig. 4 (a) and (b) shows the SCC concrete sample. In Fig. 4. (b), the chloride ion has wholly penetrated the concrete for the samples under dry and wetting cycles. In the fully saturated state (Fig. 4 (a)), the penetration rate is about 30 mm. Fig. 4 (c) and (d) is for SCC concrete samples with SCMs that have significantly reduced penetration. However, from the comparison of Figs. 4 and 5, it is clear that the cycles of drying and wetting have a significant effect on the penetration rate. Hence, the rate of penetration has increased about ten times. By comparing Fig. 4 (a) and (c), the amount of penetration has decreased by about 17 times, which shows the decrease in penetration due to the presence of SCMs.

3.4 Microstructure analysis

SEM results (provided by Hitachi SU3500) can prove the degradation mechanism of submerged samples to some

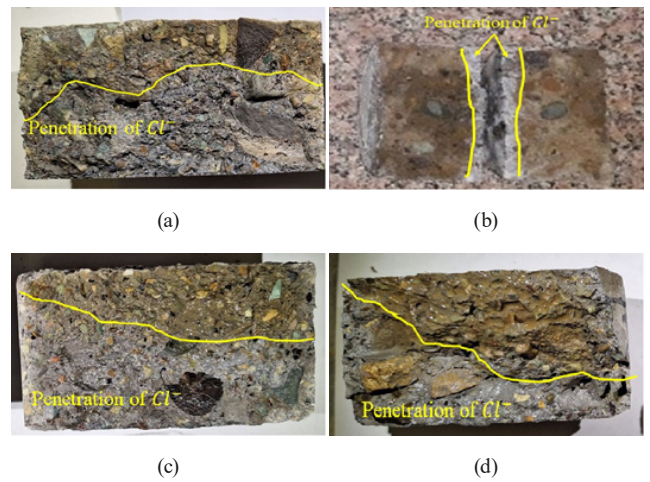


Fig. 4 Penetration Chloride after 120 days for group A: (a) SCC, (b) SL+MK+SF, (c) SL+MK, (d) SL+SF

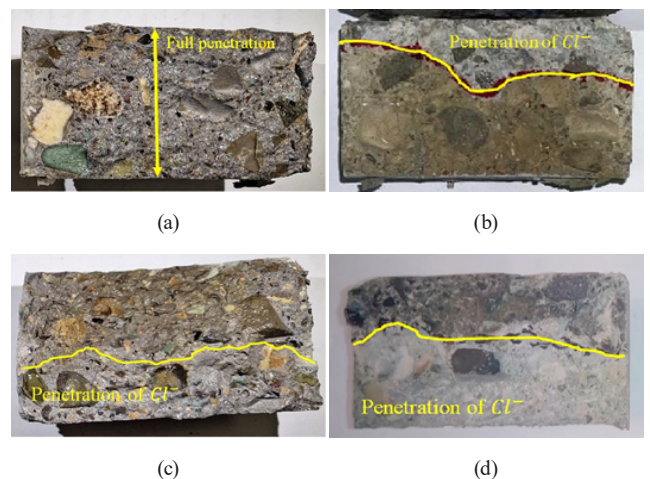


Fig. 5 Penetration Chloride after 120 days for group B: (a) SCC, (b) SL+MK+SF, (c) SL+MK, (d) SL+SF

extent. Fig. 6 (a) and (b) shows samples containing SL, MK, and SF after 120 days. As shown, there are microcracks and micropores near the aggregate. By comparing with Fig. 6 (c) and (d), which is for the SCC sample, it was found that adding SCMs in concrete reduces

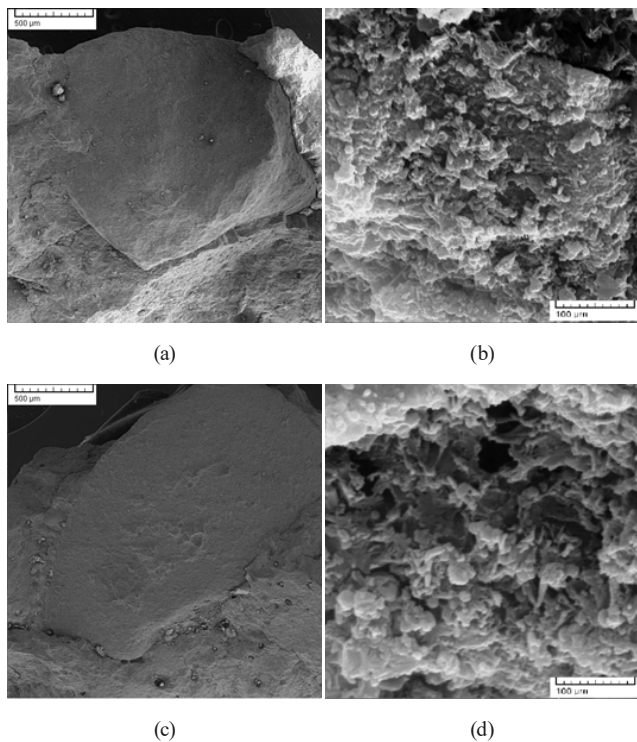


Fig. 6 SEM result of specimens after 120 days for:
 (a) SL+MK+SF (Interfacial Transition Zone (ITZ));
 (b) SL+MK+SF (C-S-H gel); (c) SCC (ITZ); (d) SCC (C-S-H gel)

the penetration of chloride ions into the concrete, which reduces the increase in volume and the creation of micro-cracks in the C-S-H gel. The SCMs filler effect, due to their particles' finer size compared to the cement particles' size, reduces the concrete pores and their connectivity. Moreover, SCMs used in this research went into pozzolanic reaction with cement hydration production, producing more C-S-H gel. However, the secondary C-S-H gel Ca/Si ratio is lower, but it increases the concrete density and reduces the pores and pores connection. Therefore, the chloride penetration into concrete reduces due to the reduction in the concrete pores.

4 Numerical development model

4.1 Determine diffusion coefficient

Considering that the diffusion coefficient changes over time, from the results of the tests performed in Table 3 for D_{28} and the deterioration coefficients and formulas in Section 2, the diffusion coefficient diagram during the structure's lifetime (50 years) is calculated and shown in Fig. 7. The Riding et al. [34] research result could be due to the effect of the additive in the early ages, and after 28 days, it is very high; that is, there are more holes and air in the regular concrete. The early concrete is relatively weak against corrosion. However, the presence of refined grains and filler in self-compacting

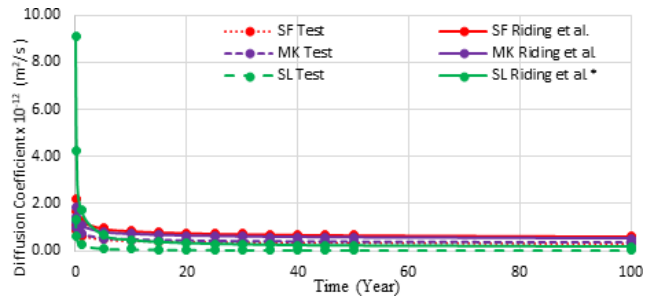


Fig. 7 The time-dependent diffusion coefficient of concrete containing a cement additive, tests, and Riding model

concrete, for samples with good mix design quality and execution, results in higher resistance of concrete against corrosion. Therefore, the increase of minerals in self-compacting concrete and the present tests, although it increases the quality of concrete and more corrosion resistance, the observed effect is less than the calculation values of Riding et al. [34].

According to the test results and comparison with the relations of Section 2, consider the diffusion coefficient of chloride ions over time of samples containing iron SL from the primary D_{28} obtained from the test and the decay coefficients similar to other admixtures and regular concrete used. The diffusion coefficient values during the structure's service life are shown in Fig. 8 for different concretes.

In Fig. 8, the penetration coefficient is highest for concrete without SCMs and lowest for concrete containing all three SCMs (SL+MK+SF), with a difference of about 13 times. When comparing individual supplementary materials, the MK sample showed the best performance, decreasing by about 2.5 times compared to the SL sample due to the increased growth of C-S-H gel in concrete. These results align with those obtained from the SEM image. When comparing samples containing two SCMs, the results indicate that the specific area of all three mixed designs is similar.

4.2 Lifetime assessment

The nature of concrete production is random, and porosity is made in the location of the aggregates. Usually, in ideal

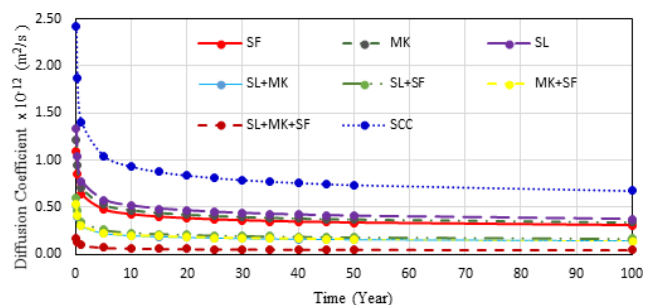


Fig. 8 Diffusion coefficient of concrete containing mineral admixtures over time

conditions, the experimental results of some samples differ slightly. By reviewing the studies done in the field of rebar corrosion, it can be seen that the collected data vary significantly, and the effective parameters don't have an exact and definite amount. The corrosion initiation time is represented in probability percent, and the corresponding reliability is calculated since there are a lot of uncertainties in the effective known parameters of rebar passive layer failure. The minimum density of the required chloride for destroying the passive layer and corrosion initiation is called the chloride threshold or C_{th} . The amount of chloride on the concrete surface, C_s , results from regression analysis of the data obtained from substantial chloride penetration and curve fitting of Fick's second law. Surface chloride density is the result of environmental conditions that the concrete presents. The most crucial factor of variations and errors in the cover size of concrete structures depends on the work environment elements such as supervision of engineers, workers, and technicians' skills. In Section 5, the probability of corrosion diagrams has been calculated and drawn based on the information in Table 5 [43–46] and the method presented in Section 2.3. Probabilistic moments and governing distribution for chloride diffusion variable in time were selected based on the mean reported in Table 4, and Eqs. (3) to (7) with lognormal distribution and coefficient of variation (COV) according to references [43–45].

Since, in some cases, a fixed diffusion coefficient is considered to estimate the life of the structure, in Fig. 9, the lifetime diagram for concrete containing single mineral admixtures is drawn with the two concrete covers specified in Table 5, which is a high estimate of the probability of corrosion for these concretes.

Depending on the criterion of corrosion initiation in probabilistic analysis, which is considered equivalent to a 10% probability of failure in some cases [30, 40] and, in some cases, 50% [46]. The lifespan of the structure can be determined. In Fédération Internationale du Béton (FIB) (International Concrete Federation), based on the design goal, different reliability indexes and, as a result, different reliability index or failure probabilities correspondence can be considered [30]. According to the expectations and

Table 5 Probabilistic moments and distribution for critical parameters of chloride corrosion [44–46]

Considerations	Mean	COV	Distribution
C_{th} (kg/m ³)	0.9	0.19	Uniform (0.6–1.2)
C_s (kg/m ³)	2.95	0.5	Lognormal
Cover (mm)	40, 30	0.5	Normal

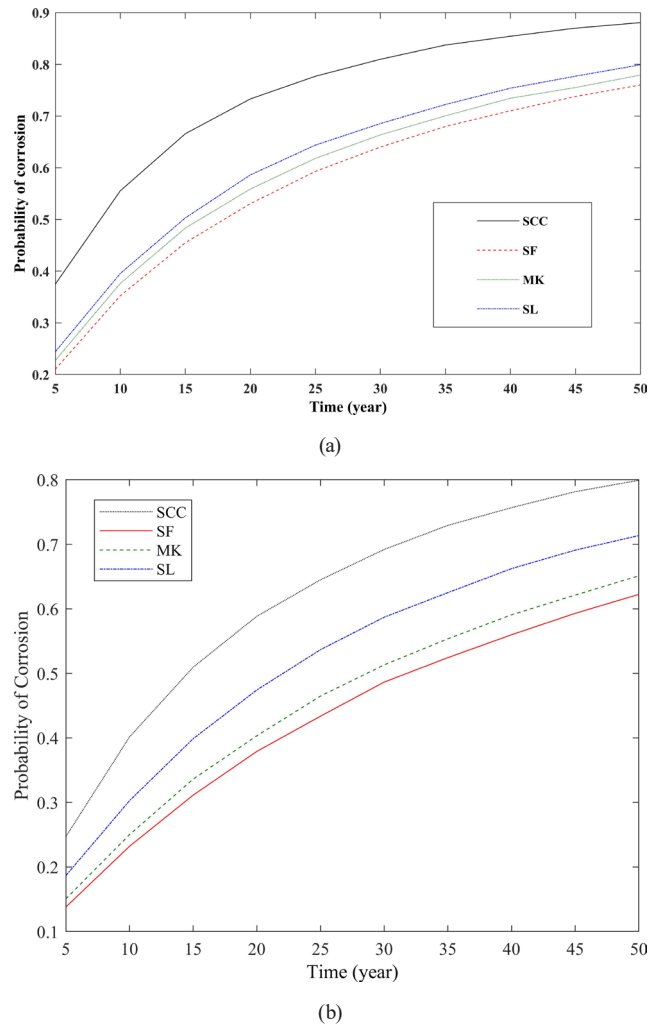
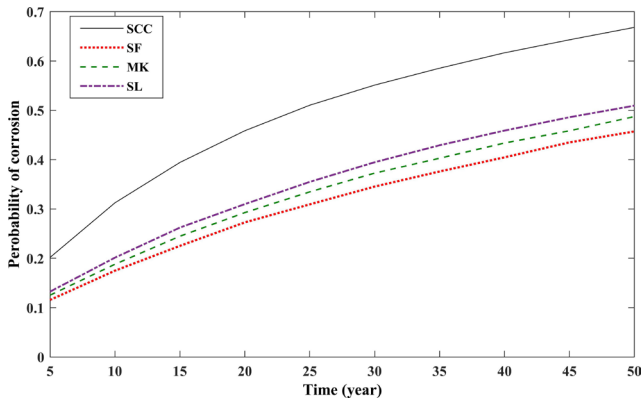


Fig. 9 Probability of corrosion initiation in different concretes with constant D_{28} for (a) Cover 30 mm; (b) Cover 40 mm

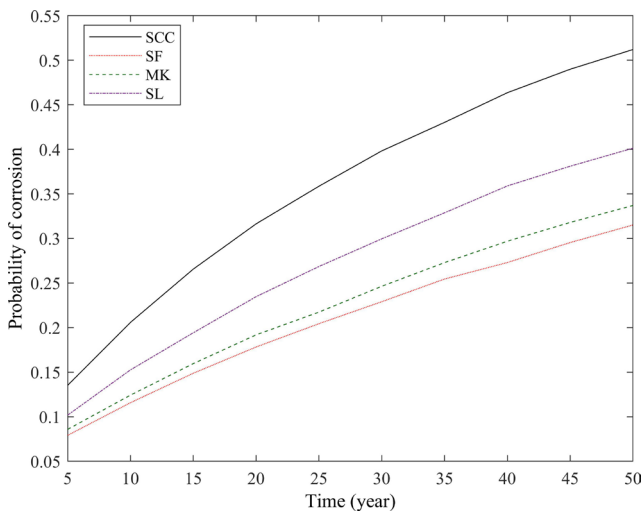
analyses of other researchers, it is clear from the graphs that in addition to the quality of concrete, choosing the right cover is also essential and has a significant impact.

All parameters should be considered in the design of the service life. Figs. 10 and 11 calculate the probability of corrosion occurrence for samples containing one and several mineral admixtures, respectively. The simultaneous use of two admixtures reduces the likelihood of corrosion by about 30% (Fig. 10).

As shown in Fig. 11, the possibility of corrosion over time will be almost halved by combining some SCMs with concrete. As a comparison between the combination of materials, it can be concluded that MK and SF performed better than the combination of SL with these two materials. The main reason can be the higher specific surface of MK and SF compared to SL. As a comparison between Fig. 11 (a) and (b), by adding 1 cm to the concrete cover, the corrosion probability has decreased by almost 40%.



(a)



(b)

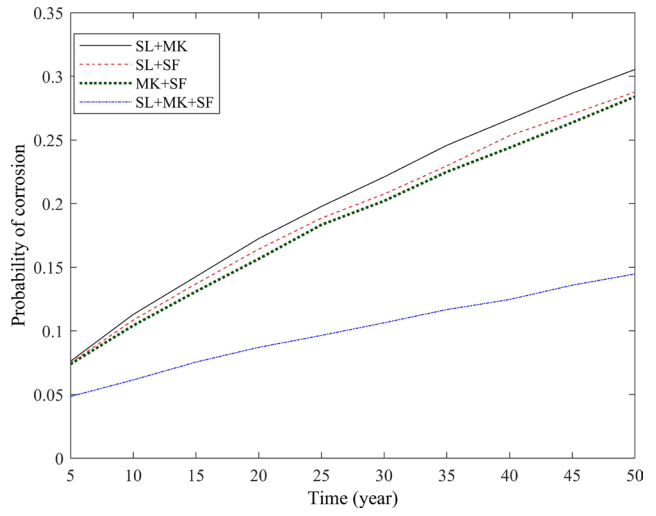
Fig. 10 Probability of corrosion initiation in different types of concretes with variable D_{28} for (a) Cover 30 mm; (b) Cover 40 mm

It should also be noted that when the combination of all three materials is used in concrete, the performance of concrete against the penetration of chloride ions has improved significantly.

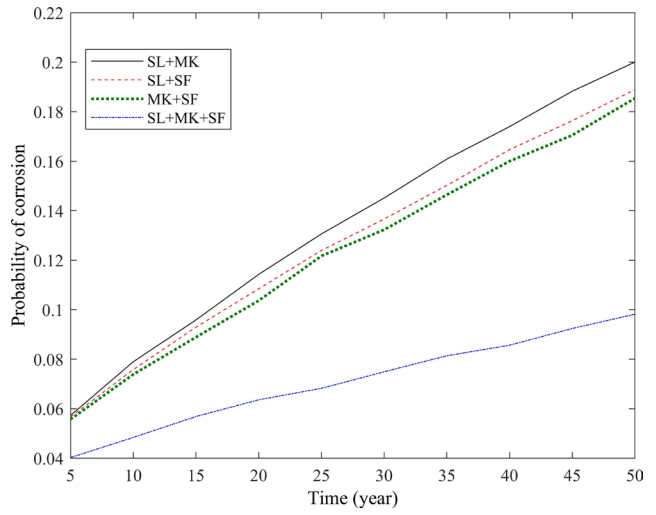
5 Conclusions

This paper used samples with different admixtures and a water-to-binder ratio 0.4 to evaluate the corrosion resistance and determine the chloride ion diffusion coefficient. Rapid migration testing has been carried out in the laboratory as part of Nord testing. Based on this examination, the distribution of chloride ions in the concrete and mineral admixtures and the results of the tests carried out were analyzed according to the HL-RF based meta-explorer algorithm used to determine the durability of concrete. The results of this study can be summarized as follows:

- The addition of SF, MK, and SL significantly reduces the permeability and chloride-ion diffusion. This could be attributed to the addition of SF causing



(a)



(b)

Fig. 11 Probability of corrosion initiation over time of concrete containing multiple SCMs for (a) Cover 30 mm; (b) Cover 40 mm

considerable pore refinement, i.e., the transformation of bigger pores into smaller ones due to their pozzolanic reaction concurrent with cement hydration.

- The addition of the mentioned SCMs together has a better effect on concrete chloride penetration resistance than using them alone. Moreover, the lowest diffusion coefficient observed in the sample contains all SCMs together as a cement replacement.
- At a given W/B ratio, for SCMs blended cementation materials, the chloride resistance and binding capacity becomes higher with the increase of SCMs' replacement ratio.
- Adding one additive decreases the probability of corrosion by about 30%. By combining two complementary cementitious materials used in concrete, the likelihood of corrosion is almost halved. The

combination of MK and SF has been better than the combination of SL with the other two materials. The main reason is the difference between the surface area of SL and MK, which has caused the diffusion coefficient to decrease by about 1.5 times.

- Adding three additives, MK, SF, and SL, to concrete decreases the probability of corrosion by about 40% after 25 years, and at 50 years, this value is about 50% compared to the case when two additional cement substances are used. This can lead to sound concrete in the life cycle.

It should be mentioned that the reliability-based model developed in this study is entirely general and does not correspond in any way particular to a specific type of concrete. However, much work still needs to be done to establish the accurate correlation between reinforcement corrosion and diffusion coefficient in concrete. Due to their significant filling effects, such as nano-TiO₂ and nano-graphene oxide in SCM concrete, nanoparticles can decrease the pores and permeability.

References

- [1] Meyer, C. "The greening of the concrete industry", *Cement and Concrete Composites*, 31(8), pp. 601–605, 2009.
<https://doi.org/10.1016/j.cemconcomp.2008.12.010>
- [2] Miller, S. A., Horvath, A., Monteiro, P. J. M. "Impacts of booming concrete production on water resources worldwide", *Nature Sustainability*, 1(1), pp. 69–76, 2018.
<https://doi.org/10.1038/s41893-017-0009-5>
- [3] Tian, Y., Zhang, G., Ye, H., Zeng, Q., Zhang, Z., Tian, Z., Jin, X., Jin, N., Chen, Z., Wang, J. "Corrosion of steel rebar in concrete induced by chloride ions under natural environments", *Construction and Building Materials*, 369, 130504, 2023.
<https://doi.org/10.1016/j.conbuildmat.2023.130504>
- [4] Karimi, A., Ghanooni-Bagha, M., Ramezani, E., Shirzadi Javid, A. A., Zabihi Samani, M. "Influential factors on concrete carbonation: a review", *Magazine of Concrete Research*, 75(23), pp. 1212–1242, 2023.
<https://doi.org/10.1680/jmacr.22.00252>
- [5] Chava, V., Rao, S., Munugala, P. K., Chereddy, S. S. D. "Effect of Mineral Admixtures and Curing Regimes on Properties of Self-Compacting Concrete", *Journal of Sustainable Construction Materials and Technologies*, 9(1), pp. 25–35, 2024.
<https://doi.org/10.47481/jscmt.1383493>
- [6] Broomfield, J. P. "Corrosion of Steel in Concrete: Understanding, Investigation and Repair", CRC Press, 2023. ISBN 9781003223016
<https://doi.org/10.1201/9781003223016>
- [7] Han, Y., Shao, S., Fang, B., Shi, T., Zhang, B., Wang, X., Zhao, X. "Chloride ion penetration resistance of matrix and interfacial transition zone of multi-walled carbon nanotube-reinforced concrete", *Journal of Building Engineering*, 72, 106587, 2023.
<https://doi.org/10.1016/j.jobe.2023.106587>
- [8] Kopeckó, K., Mlinárik, L. "The influence of different types of SCMs on microstructure and macroscopic properties of cementitious materials", *Journal of Physics: Conference Series*, 2315, 012019, 2022.
<https://doi.org/10.1088/1742-6596/2315/1/012019>
- [9] Wang, Y., Song, Y., Xue, J., Sun, X., Xue, R. "Effects of incorporating polynary SCMs on sulfate resistance and chloride impermeability of concrete considering capillary action in dry-wet cycling environment", *Construction and Building Materials*, 395, 132262, 2023.
<https://doi.org/10.1016/j.conbuildmat.2023.132262>
- [10] Cui, W., Shen, L., Ji, D., Liu, W., Wang, T., Hou, D., Shen, W., Shi, X., Tao, Y. "Mechanical performance and permeability of low-carbon printable concrete", *Journal of Sustainable Cement-Based Materials*, 2024.
<https://doi.org/10.1080/21650373.2024.2374839>
- [11] Li, C. Q., Zheng, J. J., Lawanwisut, W., Melchers, R. E. "Concrete Delamination Caused by Steel Reinforcement Corrosion", *Journal of Materials in Civil Engineering*, 19(7), pp. 591–600, 2007.
[https://doi.org/10.1061/\(ASCE\)0899-1561\(2007\)19:7\(591\)](https://doi.org/10.1061/(ASCE)0899-1561(2007)19:7(591))
- [12] Stewart, M. G., Rosowsky, D. V. "Structural Safety and Serviceability of Concrete Bridges Subject to Corrosion", *Journal of Infrastructure Systems*, 4(4), pp. 146–155, 1998.
[https://doi.org/10.1061/\(ASCE\)1076-0342\(1998\)4:4\(146\)](https://doi.org/10.1061/(ASCE)1076-0342(1998)4:4(146))
- [13] Xu, Q., Liu, B., Dai, L., Yao, M., Pang, X. "Factors Influencing Chloride Ion Diffusion in Reinforced Concrete Structures", *Materials*, 17(13), 3296, 2024.
<https://doi.org/10.3390/ma17133296>
- [14] Vera, R., Villarroel, M., Carvajal, A. M., Vera, E., Ortiz, C. "Corrosion products of reinforcement in concrete in marine and industrial environments", *Materials Chemistry and Physics*, 114(1), pp. 467–474, 2009.
<https://doi.org/10.1016/j.matchemphys.2008.09.063>
- [15] Pech-Canul, M. A., Castro, P. "Corrosion measurements of steel reinforcement in concrete exposed to a tropical marine atmosphere", *Cement and Concrete Research*, 32(3), pp. 491–498, 2002.
[https://doi.org/10.1016/S0008-8846\(01\)00713-X](https://doi.org/10.1016/S0008-8846(01)00713-X)
- [16] Zhang, J., Liu, C., Sun, M., Li, Z. "An innovative corrosion evaluation technique for reinforced concrete structures using magnetic sensors", *Construction and Building Materials*, 135, pp. 68–75, 2017.
<https://doi.org/10.1016/j.conbuildmat.2016.12.157>
- [17] Alinaghimaddah, S., Hasandoost, A. A., Karimi, A., Safiey, A. "Probabilistic study of strength and cover effects on reinforced concrete chloride corrosion", *Asian Journal of Civil Engineering*, 24(4), pp. 937–945, 2023.
<https://doi.org/10.1007/s42107-022-00543-8>
- [18] Fu, C., Jin, N., Ye, H., Liu, J., Jin, X. "Non-uniform corrosion of steel in mortar induced by impressed current method: An experimental and numerical investigation", *Construction and Building Materials*, 183, pp. 429–438, 2018.
<https://doi.org/10.1016/j.conbuildmat.2018.06.183>

- [19] Feng, W., Tarakbay, A., Memon, S. A., Tang, W., Cui, H. "Methods of accelerating chloride-induced corrosion in steel-reinforced concrete: A comparative review", *Construction and Building Materials*, 289, 123165, 2021.
<https://doi.org/10.1016/j.conbuildmat.2021.123165>
- [20] Stewart, M. G., Rosowsky, D. V. "Time-dependent reliability of deteriorating reinforced concrete bridge decks", *Structural Safety*, 20(1), pp. 91–109, 1998.
[https://doi.org/10.1016/S0167-4730\(97\)00021-0](https://doi.org/10.1016/S0167-4730(97)00021-0)
- [21] Ghanooni-Bagha, M. "Influence of chloride corrosion on tension capacity of rebars", *Journal of Central South University*, 28(10), pp. 3018–3028, 2021.
<https://doi.org/10.1007/s11771-021-4834-3>
- [22] Hasandoost, A. A., Karimi, A., Shayanfar, M. A., Ghanooni-Bagha, M. "Probabilistic evaluation of chloride-induced corrosion effects on design parameters of RC beams", *European Journal of Environmental and Civil Engineering*, 27(14), pp. 4197–4211, 2023.
<https://doi.org/10.1080/19648189.2023.2179667>
- [23] Wu, J., Xu, J., Diao, B., Jin, L., Du, X. "Fatigue life prediction for the reinforced concrete (RC) beams under the actions of chloride attack and fatigue", *Engineering Structures*, 242, 112543, 2021.
<https://doi.org/10.1016/j.engstruct.2021.112543>
- [24] Sell Junior, F. K., Wally, G. B., Teixeira, F. R., Magalhães, F. C. "Experimental assessment of accelerated test methods for determining chloride diffusion coefficient in concrete", *IBRACON Structures and Materials Journal*, 14(4), e14407, 2021.
<https://doi.org/10.1590/S1983-41952021000400007>
- [25] Khanzadeh Moradillo, M., Sadati, S., Shekarchi, M. "Quantifying maximum phenomenon in chloride ion profiles and its influence on the service-life prediction of concrete structures exposed to seawater tidal zone – A field oriented study", *Construction and Building Materials*, 180, pp. 109–116, 2018.
<https://doi.org/10.1016/j.conbuildmat.2018.05.284>
- [26] Ramezani-pour, A. A., Motahari Karein, S. M., Vosoughi, P., Pilvar, A., Isapour, S., Moodi, F. "Effects of calcined perlite powder as a SCM on the strength and permeability of concrete", *Construction and Building Materials*, 66, pp. 222–228, 2014.
<https://doi.org/10.1016/j.conbuildmat.2014.05.086>
- [27] Shafikhani, M., Chidiac, S. E. "Quantification of concrete chloride diffusion coefficient – A critical review", *Cement and Concrete Composites*, 99, pp. 225–250, 2019.
<https://doi.org/10.1016/j.cemconcomp.2019.03.011>
- [28] NORDTEST "Concrete, Mortar and Cement-Based Repair Materials: Chloride Migration Coefficient from Non-Steady-State Migration Experiments", NORDTEST, Espoo, Finland, Rep. NT BUILD 492, 1999.
- [29] Chinese Standard "GB/T 50082-2009 Standard for test methods of long-term performance and durability of ordinary concrete", Ministry of Housing and Urban-Rural Development of PRC, Beijing, China, 2009.
- [30] Schiessl, P., Bamforth, P., Baroghel-Bouny, V., Corley, G., Faber, M., Forbes, J., Gehlen, C., ..., Walraven, J. "Model Code for Service Life Design", *fib CEB-FIP*, Lausanne, Switzerland, Rep. 34, 2006.
<https://doi.org/10.35789/fib.BULL.0034>
- [31] Nord Test – Nordic Innovation Centre "Concrete, hardened: Accelerated chloride penetration", Nord Test – Nordic Innovation Centre, Oslo, Norway, Rep. 443, 1995.
- [32] ACI "Building Code Requirements for Structural Concrete (ACI 318-02) and Commentary (ACI 318R-02)", American Concrete Institute, 2002. ISBN 9780870310652
- [33] Val, D. V., Melchers, R. E. "Reliability of Deteriorating RC Slab Bridges", *Journal of Structural Engineering*, 123(12), pp. 1638–1644, 1997.
[https://doi.org/10.1061/\(ASCE\)0733-9445\(1997\)123:12\(1638\)](https://doi.org/10.1061/(ASCE)0733-9445(1997)123:12(1638))
- [34] Riding, K. A., Thomas, M. D. A., Folliard, K. J. "Apparent diffusivity model for concrete containing supplementary cementitious materials", *ACI Materials Journal*, 110(6), pp. 705–714, 2013. [online] Available at: <http://hdl.handle.net/2097/17200> [Accessed: 29 January 2024]
- [35] Oudah, F. "Time-dependent reliability-based charts to evaluate the structural safety of RC wharf decks exposed to corrosion and freeze-thaw effect", *Engineering Structures*, 283, 115887, 2023.
<https://doi.org/10.1016/j.engstruct.2023.115887>
- [36] Nagaraju, A. S. V., Kumar, R. "Reliability based service life prediction of bridges in Indian coastal region", *Structural Concrete*, 24(6), pp. 7759–7778, 2023.
<https://doi.org/10.1002/suco.202300257>
- [37] Choi, S.-K., Canfield, R. A., Grandhi, R. V. "Estimation of structural reliability for Gaussian random fields", *Structure and Infrastructure Engineering: Maintenance, Management, Life-Cycle Design and Performance*, 2(3–4), pp. 161–173, 2006.
<https://doi.org/10.1080/15732470600590192>
- [38] Hasofer, A. M., Lind, N. C. "Exact and Invariant Second-Moment Code Format", *Journal of the Engineering Mechanics Division*, 100(1), pp. 111–121, 1974.
<https://doi.org/10.1061/JMCEA3.0001848>
- [39] Rackwitz, R., Fiessler, B. "Structural reliability under combined random load sequences", *Computers & Structures*, 9(5), pp. 489–494, 1978.
[https://doi.org/10.1016/0045-7949\(78\)90046-9](https://doi.org/10.1016/0045-7949(78)90046-9)
- [40] Félix, E. F., Falcão, I. D. S., dos Santos, L. G., Carrazedo, R., Possan, E. "A Monte Carlo-Based Approach to Assess the Reinforcement Depassivation Probability of RC Structures: Simulation and Analysis", *Buildings*, 13(4), 993, 2023.
<https://doi.org/10.3390/buildings13040993>
- [41] Kaveh, A., Massoudi, M. S., Ghanooni-Bagha, M. "Structural reliability analysis using a charged system search algorithm", *Iranian Journal of Science and Technology – Transactions of Civil Engineering*, 38(2), pp. 439–448, 2014.
- [42] CEN "BS EN 12390-3:2002 Testing hardened concrete - Compressive strength of test specimens", European Committee for Standardization, Brussels, Belgium, 2002.
- [43] Jafary, A., Shayanfar, M. A., Ghanooni-Bagha, M. "Investigation on the corrosion initiation time of reinforced concrete structures at different distances from the Sea", *Amirkabir Journal of Civil Engineering*, 55(2), pp. 389–406, 2023.
<https://doi.org/10.22060/ceej.2022.20005.7312>

- [44] Stewart, M. G., Al-Harthy, A. "Pitting corrosion and structural reliability of corroding RC structures: Experimental data and probabilistic analysis", *Reliability Engineering & System Safety*, 93(3), pp. 373–382, 2008.
<https://doi.org/10.1016/j.res.2006.12.013>
- [45] Nogueira, C. G., Leonel, E. D. "Probabilistic models applied to the safety assessment of reinforced concrete structures subjected to chloride ingress", *Engineering Failure Analysis*, 31, pp. 76–89, 2013.
<https://doi.org/10.1016/j.engfailanal.2013.01.023>
- [46] Saassouh, B., Lounis Z. "Probabilistic modeling of chloride-induced corrosion in concrete structures using first- and second-order reliability methods", *Cement and Concrete Composites*, 34(9), pp. 1082–1093, 2012.
<https://doi.org/10.1016/j.cemconcomp.2012.05.001>